XVII[th] World Congress of the International Commission of Agricultural and Biosystems Engineering (CIGR)

Hosted by the Canadian Society for Bioengineering (CSBE/SCGAB)
Québec City, Canada June 13-17, 2010

AERODYNAMIC MODELING OF WINDBREAKS IN SAEMANGEUM RECLAIMED LAND

J. P. BITOG[1,2], I-B. LEE[1], S-W. HONG[1], H-S. HWANG[1], I-H. SEO[1], K-S. KWON[1], J-S. CHOI[1], S-Y. SONG[1]

1 Department of Rural Systems Engineering and Research Institute for Agriculture and Life Sciences, College of Agriculture and Life Sciences, Seoul National University, Gwanakgu, 151-921 Seoul, Korea, iblee/ identi0607/ wooni91/siwbest0@ snu.ac.kr
2 Department of Agricultural Engineering, College of Engineering, Nueva Vizcaya State University, 3700 Bayombong, Nueva Vizcaya, Philippines, jessppb2001@yahoo.com

CSBE100677 – Presented at 8[th] World Congress on Computers in Agriculture (WCCA)

ABSTRACT This paper discusses the quantitative effect of windbreaks on wind velocity in the reclaimed land at Saemangeum in South Korea. The effectiveness of windbreaks to reduce the velocity to prevent the generation and diffusion of dust are very critical. Using CFD simulations, the effects of porosity, height, and distance between the adjacent fences as well as the effect of tree windbreaks were investigated. A wind tunnel test was conducted and data gathered were used to develop and validate the CFD models. From the experiments and CFD simulations, the overall percentage difference of the measured velocities was 7.20% which is acceptable to validate the CFD models. In the case of tree windbreak simulation, the methodologies to model the real effect of tree windbreak were conducted and compared such as the application of tree porosity, inertial resistance and input velocity. Results have shown that a windbreak fence with porosity of 0.2 and a height of 0.6 m and constructed in array at 6 m distance between them is necessary. Initial simulation of tree windbreak also has shown that the effect of trees on flow fields using inertial resistance can be appropriate to model the real condition, although this should still be strongly validated in field studies or in wind tunnels. This study proved that CFD can be an effective tool to investigate wind flow affected by windbreaks.

Keywords: Computational fluid dynamics (CFD), Porosity, Tree modeling, Fence

INTRODUCTION The sandy land known as Saemangeum is the biggest land reclamation project in South Korea. The project reclaimed 11,800ha of freshwater lake and 28,300ha of land. However, the generation of dust from and its diffusion to the surrounding areas has become a problem. This happens because of high velocity in the area. The absence of natural barriers, which control velocity, and the flat topography of Saemangeum have worsened the problem. Hwang et al. (2006) measured the amount of dusts in the area with respect to the vertical height and found substantial amount of dusts approximately 700μg at a height of 0.80m from the ground. The value was doubled when measured at 0.4m height, showing significant amount of dust near the ground. The dusts also contain high amount of sodium chloride (NaCl) which is very harmful to plants.

To prevent the generation of dust, artificial windbreak fences made of bunches of rice straw and coconets were constructed (Fig. 1). The use of natural windbreaks such as trees were also being planned to be planted in the affected areas to prevent the entry of the dust. Trees have been very effective to protect farmlands for crops and livestock production, to control soil erosion, etc. Generally, the basic functions of windbreaks are to reduce wind velocity and change its direction around windbreaks. The functions depend on the height (*H*), width or thickness, porosity and orientation of the windbreaks.

Windbreaks provide a sheltering effect by decreasing the wind speed in large zones behind the fences (Santiago et al., 2007). A review of the effect of windbreak structures on wind flow was done by Heisler and Dewalle (1988). They found that the efficiency of windbreaks greatly depends on the type, height and shape, and porosity of the windbreak. The most influential, however is porosity. Low porosity can produce high maximum reductions. They can create more turbulence downwind than the medium and high porosity windbreaks. Porosity can be described by optical porosity β and aerodynamic porosity α. The optical porosity is the ratio of the open surface to the total surface of the windbreak. The aerodynamic porosity α is the ratio of mean wind speed at leeward from the bottom to the top of the windbreak to that upwind before windbreak interference. Guan et al. (2003) suggested the relationship between the porosities to be $\alpha = \beta^{0.4}$.

Windbreaks normally have the shape of a rectangle and usually the higher the windbreak, the larger the protected zone. Horizontal distances and wind speed are usually expressed in terms of height of the windbreak (*H*) and approach wind speed ($U_{approach}$), respectively. Windbreak influence extends from -5*H* (windward) to 30-35*H* (leeward). Minimum wind speed is achieved in the near lee, at distances of 4-6*H*. Further leeward, at about 20*H*, wind speed recovers to 80% of the approaching wind speed. For very dense windbreaks, the wind profile shows a lower minimum wind speed but a faster wind speed recovery near the lee (between 0*H* and 10*H*), compared to a porous windbreak (Eimern et al., 1964; Heisler and Dewalle, 1988; Plate, 1971; Ucar and Hall, 2001; Vigiak et al., 2003).

Although a number of experimental studies on dust diffusion had been conducted, a thorough investigation on the quantitative effect of the constructed fences as well as tree windbreaks has yet to be done. Field experiment for this kind of research is necessary but may take some time and require big amount of money and intensive labor given the site's vast land and variable climate. Due to the complex nature of Saemangem reclaimed land, at this time, it would be wise to conduct model simulation.

The advent CFD in the 70s and its continuous development has paved the way to study aerodynamic phenomena in a more realistic way. The application of CFD technique in studying the effect of several windbreak structures had been conducted (Dong et al., 2007; Li et al., 2007; Santiago et al., 2007; Qiu et al., 2004; Wilson and Yee, 2003). The analysis of the flow characteristics of these studies were based on the use of the windbreaks with emphasis on the effects at the lee. In the Saemangeum where prevention of dust generation and diffusion is the main goal, quantitative reduction on velocity in the dust source areas is a significant research to undertake. Conventionally, this type of study can be done in wind tunnels and in field experiments. However, such approaches are always expensive and time consuming (Li et al., 2007). Using CFD technology provides a quick and economical alternative to wind tunnel test approach for practical use with adequate computer expertise.

The objective of the study is to measure the quantitative effect of fences as well as trees on wind flow. In case of the artificial fences, the effect of porosity, height and distance between them is analyzed and the optimum parameters of the fence suitable in the area are determined. In the tree simulation, the quantitative effect of trees in reducing wind velocity as well as the extent of its effect in the horizontal direction is determined.

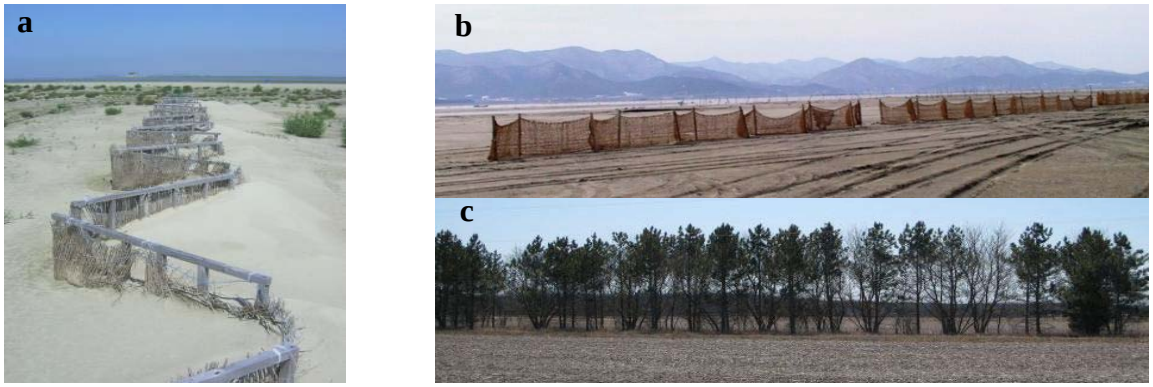

Fig. 1. (a) Windbreak fence made from rice straw and (b) fence made from coconets which were installed in Saemangeum area; and (c) trees as windbreak.

MATERIALS AND METHODS

Wind Tunnel

A wind tunnel is a research tool developed to assist in studying the effects of air moving over or around solid objects, or vice versa. The approach is focused on producing controlled airflow to study its effect on objects moving through the air or the effects of moving air on stationary models. A wind tunnel is an economical and safe method to collect valid data. However, the dimensional difference between the full-scale and small-scale models, airflow characteristics, etc., must be carefully managed to ensure accuracy. A wind tunnel at the Institute of Agricultural Engineering (IAE) of Korea was used.

Computational Fluid Dynamics (CFD)

CFD is a powerful tool to study fluid flows where computers and numerical techniques to solve problems involving fluids are used. The CFD technique solves the Navier-Stokes equations within each cell of the domain. The mass, continuity, and energy conservation equations (Eqs. (2), (3), and (4), respectively), were used (Fluent manual, 2006).

$$\frac{\partial \rho}{\partial t} + \frac{\partial}{\partial x_i}(\rho \mu_i) = S_m \tag{2}$$

$$\frac{\partial \rho}{\partial t} + (\rho \mu_i)\frac{\partial}{\partial x_i}(\rho \mu_i \mu_i) = -\frac{\partial p}{\partial x_i} + \frac{\partial \tau_{ij}}{\partial x_j} + \rho g_i + F_i \tag{3}$$

$$\frac{\partial \rho}{\partial t} + (\rho h)\frac{\partial}{\partial x_i}(\rho \mu_i h) = \frac{\partial}{\partial x_i}\left(K \frac{\partial T}{\partial x_i}\right) - \frac{\partial}{\partial x_i}\sum_j h_j J_i + \frac{\partial \rho}{\partial t} + \mu_i \frac{\partial p}{\partial x_i} + \tau_{ij}\frac{\partial \mu_i}{\partial x_j} + S_h \tag{4}$$

where: F_i: force vector (N m^{-3}); g_i: gravitational acceleration (m s^{-2}); J_i: diffusion flux (kg m^{-2} s^{-1}); h: enthalpy (J kg^{-1}); K: conductivity (W m^{-1} K^{-1}); p: pressure (Pa); S_m: mass

source (kg m^{-3} s^{-1}); S_h: entropy (J K^{-1}), *T*: temperature (K); t: time (s); μ_i: velocity (m s^{-1}); x_i: length (m); ρ: fluid density (kg m^{-3}); τ_{ij}: stress tensor (Pa).

Gambit (ver. 2.2, N.H., Fluent, Inc.) was employed for the pre-processing of the models, in which the final geometries were designed and developed. The CFD solver Fluent (ver. 6.2, N.H., Fluent, Inc.) was used as the module to perform the CFD calculation.

Advantages of simulation in this study are: a) an artificial condition depicting the real atmospheric conditions can be set-up; b) the effect of various fence and tree configurations can be individually studied; c) the effect of porosity can be easily modelled and investigated; d) wind flow characteristics, and how are they affected by the various parameters, can be visualized; and e) this technique saves time, money, and effort.

Experimental procedure

Wind tunnel experiment

A wind tunnel experiment was conducted to determine the theoretical logarithmic velocity profile. This was achieved by setting up wooden blocks at the test section of the wind tunnel to create turbulence. Trial and error was used to determine the appropriate number, size and arrangement of blocks at the test section. The velocity profile was measured at a distance of 120 cm after the last formation of blocks. After the desired profile was obtained, the fences were set up and arranged according to the case to be tested. The summary of cases is presented in Table 1. For similarity of velocity, Froude number was used as (Eq. (1); Simiu and Scalan, 1996; Cook, 1997) where: *V* is the velocity (m s^{-1}); *g* is th gravitational acceleration (m s^{-2}), and *B* is geometrical dimension of the structure (m).

$$\left(\frac{V^2}{gB}\right)_{model} = \left(\frac{V^2}{gB}\right)_{full} \quad (1)$$

For similarity of dimensions, 1/5 scale was chosen to provide enough space for allowing an airflow similar to the actual airflow. Solid materials made of plastic 0.01 m thick and 2 m long were used to model the fences. The height of the model fences and the adjacent distance between them were 12, 16, and 20 cm and 40, 80, and 120 cm, respectively.

CFD simulations

Several 3-D geometries were designed from Gambit with varied mesh value from coarse to dense. In the calculation, the RNG κ-ε turbulence model, which is very popular for general CFD simulations (Launder and Spalding, 1972), was employed. The RNG κ-ε equations shown in Eqs. (5) and (6) were derived from the application of a rigorous statistical technique (Renormalization Group Method) to the instantaneous Navier-Stokes equations (Fluent manual, 2006). All simulations performed assumed steady-state conditions, with the inlet airflow assumed to be turbulent and incompressible.

$$\rho\frac{Dk}{Dt} = \frac{\partial}{\partial x_i}\left(\alpha_k \mu_{eff}\frac{\partial_k}{\partial x_i}\right) + G_k + G_b - \rho\varepsilon - Y_M \quad (5)$$

$$\rho\frac{D\varepsilon}{Dt} = \frac{\partial}{\partial x_i}\left(\alpha_\varepsilon \mu_{eff}\frac{\partial_\varepsilon}{\partial x_i}\right) + C_{1\varepsilon}\frac{\varepsilon}{k}(G_k + C_{3\varepsilon}G_b) - C_{2\varepsilon} - \rho\frac{\varepsilon^2}{k} - R \quad (6)$$

where $C_{1\varepsilon}$ and $C_{2\varepsilon}$: constant (1.42 and 1.68, respectively); $C_{3\varepsilon}$: $\tanh \left|\frac{\mu_1}{\mu_2}\right|$ (μ_1 and μ_2 are the flow velocities parallel and perpendicular to the gravitational vector, respectively); t: time (s); ε: dissipation rate ($m^2\ s^{-3}$); k: kinetic energy ($m^2\ s^{-2}$); ρ: density ($kg\ m^{-3}$); μ_{ff}: viscosity (m^2 s); x_i: length (m); G_k: generation of turbulent kinetic energy due to the mean velocity gradients ($kg\ m^{-1}\ s^{-2}$); G_b: generation of kinetic energy due to the buoyancy ($kg\ m^{-1}\ s^{-2}$); α_k: kinetic energy due to the mean velocity gradients ($kg\ m^{-1}\ s^{-2}$); α_ε: kinetic energy due to buoyancy ($kg\ m^{-1}\ s^{-2}$); R: gas-law constant ($J\ kgmol^{-1}\ K^{-1}$); Y_M: contribution of the fluctuating dilatation in compressible turbulence to the overall dissipation rate ($kg\ m^{-1}\ s^{-2}$).

The velocity profile from the wind tunnel test, the turbulent kinetic energy (κ) and dissipation rate (σ) were the inputs used in the model. The κ and σ values at different heights were calculated from the measured wind tunnel data using Eqs. (7) and (8) (Fluent manual, 2006) where C_μ is a constant specified in the turbulence model (0.09); U_{avg} is the average velocity ($m\ s^{-1}$); I is the turbulence intensity; l is the turbulence length scale. The general flow chart of the CFD process is shown in Fig. 2.

$$k = \frac{3}{2}(U_{avg} I)^2 \tag{7}$$

$$\sigma = C_\mu^{3/4} \frac{k^{3/2}}{l} \tag{8}$$

For the simulation of fences, three fence heights (A_1: 0.6, A_2: 0.8, and A_3: 1.0 m), three distances between the adjacent fences (B_1: 2, B_2: 4, and B_3: 6 m), and four fence porosities (C_1: ε = 0, C_2: ε = 0.2, C_3: ε = 0.4, and C_4: ε = 0.6) were the parameters varied. This gave a total of 36 model cases. The measured wind velocities from CFD simulations and wind tunnel experiments were compared and analyzed. After establishing the reliability of the CFD models, simulation of the remaining cases followed.

The effect of the simulated cases were evaluated by comparing velocities measured at different height of the inlet to the velocities measured at different height in between the adjacent fences and at the leeward. First, the percentage decrease of velocity was calculated at every height, and then the percentage decrease in every measuring location was determined by taking the average of the percentage decreases at every height. The percentage decrease up to a height of 0.6 m from the ground surface was used as the base height. Finally, the overall average percentage decrease was determined by taking the average of the percentage decrease at each measuring location.

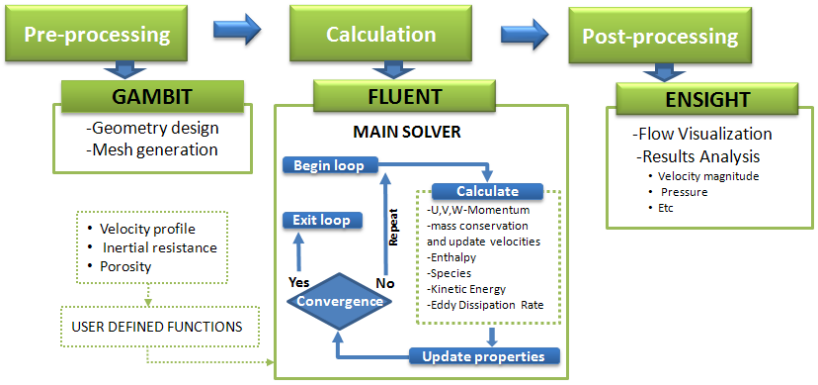

Fig. 2. General flowchart of the CFD process.

RESULTS AND DISCUSSION

Vertical wind velocity profile from wind tunnel test

The trial and error approach in determining the number, size and the arrangement of the wooden blocks was very tedious to conduct but very necessary to obtain accurate results. This procedure took at least 2 days to come up with the desired result. A total of 73 wooden blocks comprising of 23-7x7 cm, 30-5x5 cm, and 30-3x3 cm blocks was determined to create the desired logarithmic wind profile.

Table 1. Cases tested in the wind tunnel.

Case*	Combination			
	Actual dimension (m)		Scaled dimension (cm)	
	Fence height	Distance b/t fence	Fence height	Distance b/t fence
1	0.6	2.0	12	40
2	0.6	4.0	12	80
3	0.6	6.0	12	120
4	0.8	2.0	16	40
5	0.8	4.0	16	80
6	0.8	6.0	16	120
7	1.0	2.0	20	40
8	1.0	4.0	20	80
9	1.0	6.0	20	120

*Cases 1 to 9 were modelled as solid fences therefore the porosity is zero.

Development and validity of the 3-D CFD models

The 3D CFD models were developed based on the wind tunnel tests results. The velocities from the models were compared against the velocities measured from wind tunnel. The total length of the models for the cases with 2, 4, and 6m distances between the fences were 15, 19, and 23m, respectively. The height was uniform at 6m, and the width of the fence was 0.5m with both ends simulated as symmetrical. The thickness of the fences was 0.04 m to allow at least two mesh counts within the fence. To model the fences, the volumes were zoned as solid for solid fences and liquid for porous fences.

The average percentage differences of the measured velocities from wind tunnel and simulation results were determined and the computed maximum and minimum differences were 12.79% and 3.20%, respectively. The overall difference was computed to be 7.20% which is acceptable to establishing the reliability of the CFD models.

A comparison of the wind profiles measured from wind tunnel test and the simulation results of cases 1 is presented in Fig 3. The figures show a similar trend in all measuring points, which strengthened the reliability of the simulations. A good agreement between the wind tunnel test and simulation is also observed for the remaining cases.

Simulation analysis

Fence windbreaks

The highest percentage decrease in velocity was attained at 0.2 porosity, 0.8m height and 2m distance between the adjacent fences. The lowest percentage decrease was attained at

0.6 porosity, 0.6m height and 2m distance. The highest and lowest percentage decrease was computed to be 93% and 22% respectively (Fig. 4). Generally, a higher percentage decrease is observed between fence 2 and fence 3. This makes sense because the wind velocity was already reduced when the wind passed through the first and second fences. The effect of the porosity, height, and distance is presented in the following sections.

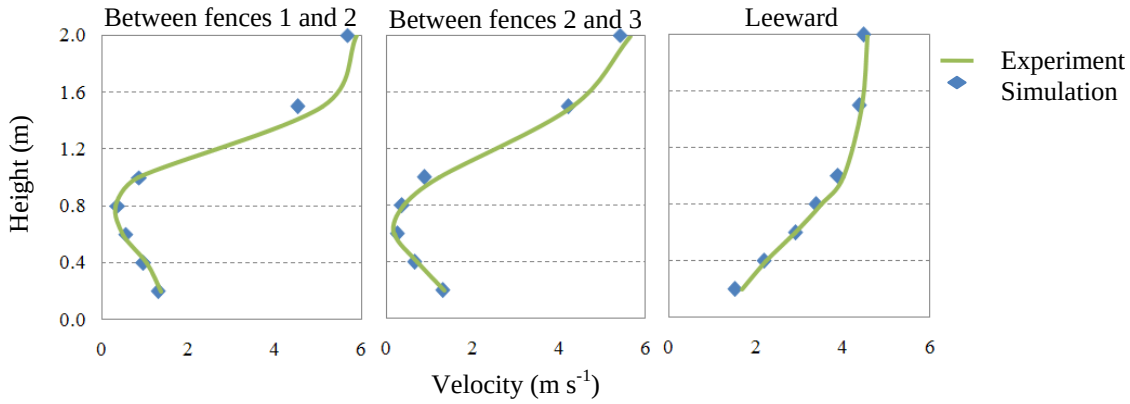

Fig. 3. Comparison of vertical wind profiles measured from wind tunnel tests and simulations for Case 1. Similar results were obtained for the other remaining cases.

Simulation results revealed that a porosity of 0.2 gave the largest decrease in wind velocity (75-93%), regardless of height and distance between the adjacent fences. The quantitative effect of the fences with 0, 0.4, and 0.6 porosities were 50-85%, 60-80%, and 20-45%, respectively (Fig.4). Simulation showed that the solid fences caused re-circulating flows in the region bounded by the adjacent fences and at the leeward. This counteracts the direction of flow, creating more turbulence causing a lesser reduction in velocity. This scenario can also generate more suspended dusts. No re-circulating flows are observed when the fence porosity is 0.2, and the velocity is significantly reduced. Comparing the wind velocities at the bounded regions at 0.3 m height, the velocities at regions bounded by fence 1 and fence 2 is slightly higher. However, the velocities are still lower than the threshold velocity. No re-circulating flows were observed with fence porosity values of 0.4 and 0.6; however, the decrease in velocity is very minimal, and the airflow penetrating the fences is dominant.

For the solid fences, the effect of fence height in reducing the velocity is decreased as the height is increased. However, this is not true for porous fences for which no significant difference in the reduction of velocity is observed; therefore, it can be argued that fence height has no significant effect in reducing velocity at regions bounded by the fences. If the sheltering effect at the horizontal direction is the concern, the fence height is one of the main factors. Studies have shown that the horizontal effect can be proportional to the windbreak height, and the effect can go as far as 50*H* to the lee, and rarely, even farther with a reduction of 20% or more may extend to about 25*H* from the windbreak (Heisler and Dewalle, 1988). Focusing on fences with 0.2 porosity, the decreases in wind velocity for the 0.6, 0.8, and 1.0m fence heights were 84%, 89%, and 81%, respectively (Fig.4).

The velocity only decreased gradually when the distance between the adjacent fences is increased, regardless of porosity or height. Focusing on 0.2 porous fences, the velocity at regions bounded by the fences is greatly reduced regardless of the fence height. The

decrease in velocity for 2, 4, and 6 m distances were 91%, 85%, and 79%, respectively (Fig. 4). It was initially thought that the effect of distance would be significant because the gap between the fences can allow the wind to regain strength before approaching the next fence; however, the results showed otherwise. The successive difference is only 3-5% with higher reduction observed in the first fence. In general, in an array of fences, the efficiency of successive windbreaks is less than that of the first windbreak.

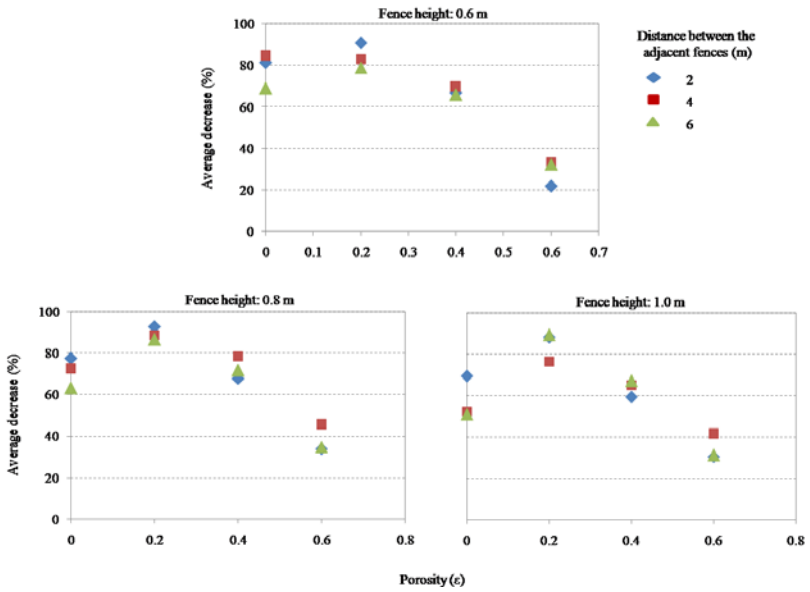

Fig. 4. Average percentage decrease in wind velocity as influenced by porosity, height, and distance.

Tree windbreaks

Several approaches to model the effect of tree windbreak were conducted such as the application of porosity, velocity profile and inertial resistance. Initial simulation have shown that the use of porosity and velocity profile has some limits in capturing the effect of trees on wind flows while inertial resistance shows promising results. Optical porosity of different tree species were measured by Loeffler et al. (1992) and found out that porosity within the tree is different at every height and using the average porosity is not enough to show the effect of tree on wind flow. Making a velocity profile within the tree is another option but limited if successive trees are included. The velocity profile is measured using the equation (9) proposed by Zhu et al. (2004) where the profile is dependent on the wind velocity outside the tree crown. If successive trees are included in a row, this equation cannot be applied because the velocity profile in the successive trees is dependent on the velocity at the leeward of the first row of trees.

$$U_{\mathrm{in(z)}} = U_{\mathrm{out(z)}} \exp\left[-\alpha_s \left(1 - \frac{z}{H}\right)\right] \tag{9}$$

where z: interest height in the canopy (m); H: height of the canopy top (m); $U_{\mathrm{out(z)}}$: wind speed outside the crown (ms^{-1}); α_s: constant (dimensionless).

Using inertial resistance show some promising results where the effect of trees in wind velocity can be correctly simulated. Inertial resistance can also be applied to all trees if additional row of trees are included. Presented in Fig. 5 is a contour profile of wind flow when porosity, velocity profile and inertial resistance were used.

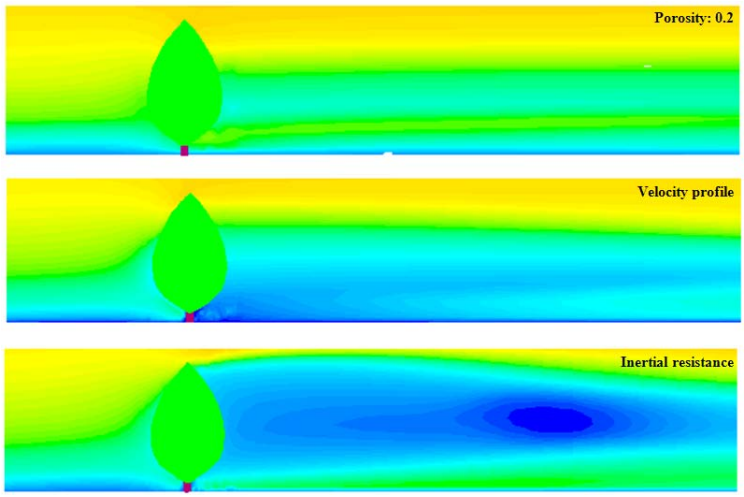

Fig. 5. Contour of wind velocity using different methods of simulating the effect of trees on wind flow.

Presented in Fig. 6 are the average velocities measured at 1.5 m height for one-row, two-rows and two-rows alternating tree windbreaks when inertial resistance was used. It is very clear that alternating two-rows of trees gives the highest decrease. This is absolutely true in actual situation because the alternating arrangement allows the windbreak to close up faster. The prevailing wind is slowed down at ground level, but wind is still able to pass through the trees which depend greatly on the inertial resistance. Stronger air currents stay high above the trees.

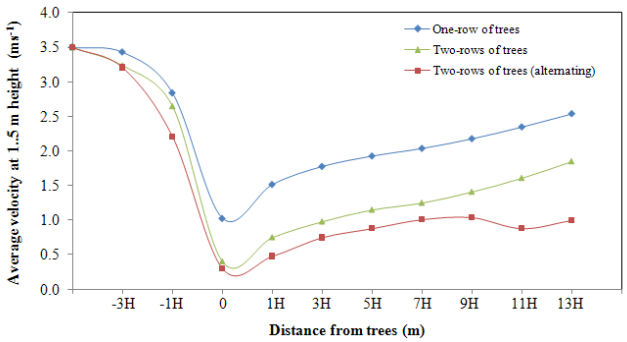

Fig. 6. Comparison of average measured wind velocity for one-row, two-rows and two-rows of tree windbreaks.

CONCLUSIONS

In this study, the quantitative reduction of wind velocity for fence windbreaks and tree windbreaks were measured. In case of the fences, a porosity of 0.2 was found the optimum. This is in agreement with the study by Li et al. (2007) where high-density windbreaks (0.2-0.3 porosity) are recommended to reduce wind speed over large areas. The effect of fence height at regions bounded by the adjacent fences was not significant. However, this finding is not true if the horizontal extent of the windbreak effect is to be considered, because fence height is a major factor and the location of measuring the wind velocities is focused and extended on the horizontal leeward plane. It is usually assumed that the horizontal effect of a windbreak is proportional to the windbreak height, and the effect can go as far as 50 *h*, where *h* is the fence height. Since no significant differences

were found on the effect of fence height, the 0.6 m fence height is recommended for practical reasons. The effect of the distance between adjacent fences was found to significantly decrease the wind velocity to approximately 75% at 0.2 porosity, therefore, constructing fences in an array, 6 m apart, is very reasonable and appropriate.

Initial simulation results have also shown that the use inertial resistance can correctly simulate the effect of tree windbreaks on wind flows. Two-rows of trees alternating show the highest decrease in wind velocity. However, this should still be validated by conducting field experiments or wind tunnel test.

Finally, in this study, it was shown that the CFD technique has the potential to be a very powerful tool for investigating wind flow characteristics as affected by artificial windbreaks and natural windbreaks such as trees. The developed skills and expertise in using CFD to study this kind of research would lead us to investigate the effect other natural wind barriers, such as crops, which were grown in the area.

REFERENCES

Cook, N. (1997). The Designer's guide to wind loading of building structures: Part 2. Oxford, U.K., Butterworth.

Dong, Z., Luo, W., Qian, G., Wang, H. (2007). A wind tunnel simulation of the mean velocity fields behind porous fence. Agriculture & Forest Meteorology 146, 82-93.

Fluent manual (2006). Fluent Co. New Hampshire, USA.

Heisler, G.M., Dewalle, D.R. (1988). Effects of Windbreak structure on Wind Flow. Agriculture, Ecosystems and Environment, 22/23, 41-69.

Hwang, H.S., Lee, I.B., Chang, P.W., Hong, S.W., Seo, I.H., Lee, S.Y. (2006). Monitoring of dust emission at a reclaimed land and its 3-D aerodynamic modeling. ASABE paper No. 062055. St. Joseph, Mich., ASABE.

Launder, B.E., Spalding, D. B. (1972). Mathematical models of turbulence. Academic Press Inc. (London) Limited Paper, pp 169.

Lee, I.B., Sase, S., Sung, S.H. (2007). Evaluation of CFD accuracy for the ventilation of a ventilated broiler house. Japan Agricultural Research Quarterly 41 (1), 53-64.

Lee, I.B., Kang, C., Kim, G., Heo, J., Sase, S. (2004). Development of vertical wind and turbulence profiles and wind tunnel boundary layers. Transactions of the ASAE Vol. 47(5), 1717-1726.

Li, W., Fan, W., Bell, S. (2007). Simulating the sheltering effects of windbreaks in urban outdoor open space. Wind Engineering and Industrial Aerodynamics 95,533-549.

Qiu, Y. G., Lee, I.B., Shimizu, H., Gao, Y., Ding, G. (2004). Principles of sand dune fixation with straw checkerboard technology and its effect on the environment. Journal of Arid Environments 56, 449-464.

Santiago, J.L., Martin, F., Cuerva, A., Bezdenejnykh, N., Sanz-Andres, A. (2007). Experimental and numerical study of wind flow behind windbreaks. Atmospheric Environment 41, 6406-6420.

Simiu, E., Scanlan, R.H. (1996). Wind effects on structures. John Wiley and Sons, N.Y.

Wang, K. (1991). Studies on sand dune stabilization in the shapotou area. Research on Desert Control 2, 13-26.

Wilson, J.D., Yee, E. (2003). Calculation of winds disturbed by an array of fences. Agricultural and Forest Meteorology 115, 31-50.